Paul Ray Richard

Soil Mechanics of Flood Control

Introduction

Soil mechanics plays and important role in the design and performance of flood control systems. Flood protection levees are often embankments made entirely from locally available soil. Other structural elements such as control structures, diversions and monitoring stations must have a resilient foundation. The objective of this learning module is to summarise soil behaviour concepts, including soil stability, groundwater seepage and interaction with structures. The first section is a very brief review of basic soil mechanics applied to flood control. The sections that follow address seepage through and under embankments and slope stability of embankments.

From the perspective of a non-expert, the subject of soil mechanics may seem unimportant, or merely a pedestrian exercise. However, when viewed from a failure perspective (Figure 1), its importance should be quite clear. The two largest categories are "Quality Problems" and "Overtopping". The Quality Problems category is broken down into the sub-categories shown; mostly dealing with soil. Overtopping can also be worsened by soil problems where the soil at the crest erodes and generates much more flow, and possibly failure of the entire embankment. The topics of this learning module should be obvious, given the main causes of failure: Piping (seepage) and Sliding (slope stability).

Case studies

Case studies of field performance (both successes and failures) are critical to understanding how embankments perform. Monitoring projects during construction, then during operation give insight into the behaviour of the levee or hydraulic control system, not just a single component or material. This is often overlooked by designers (and professors) who are more often focused on specific aspects of a design or performance of a particular material. Full-scale monitoring is very difficult. It is expensive, time-consuming and often boring. The monitoring program is at the mercy of nature[1] who rarely cooperates. Forensic studies of failures are also useful since the engineer knows that the system has definitely failed. By back-calculating stability or seepage analyses, one may gain

[1] I recall two such projects where funding lasted for three years. For both projects, the region experienced drought conditions for the entire duration of the research. It is indeed difficult to gather flood control data when there is no water. Three years later, one of the project locations experienced a 100-year event, destroying much of the instrumentation. We could only run forensics on the damage we found.

https://doi.org/10.36250/01052_09

insight into the actual (versus predicted or designed) performance. Lessons from failures constitute a large percentage of geotechnical knowledge gained in the field.

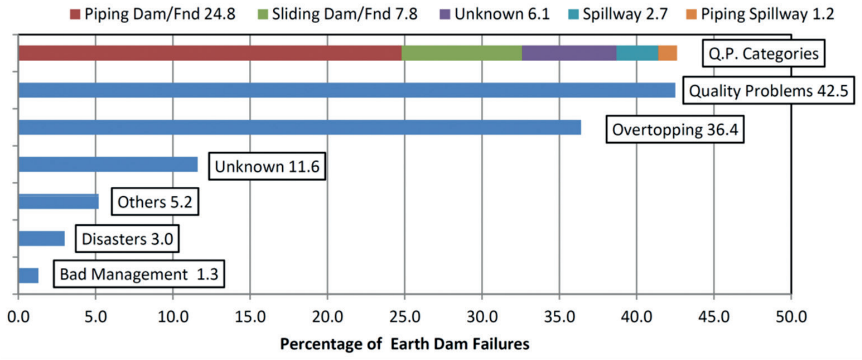

Figure 1. Causes of earth dam failures from a database of 591 studies (top bar is subdivided into specific categories) [26]

Case Study – Overtopping

Tous Dam, Spain was a 70 m high rockfill dam with a central clay core located near Valencia, Spain, failed due to overtopping [7,17]. It was designed and built as a flood defence structure and was also used for flow regulation and irrigation. Construction started in 1958 as a concrete dam 80 m tall but geotechnical conditions forced a stoppage in 1964. The design was modified and resumed in 1974 where the central embankment now consisted of a clay core with rockfill cover and finished in 1978. Final dimensions were 70-m tall and 400-m crest length. The emergency spillway used radial gates with a capacity of 7,000 m^3/s while the service spillway had a capacity of 250 m^3/s. During 19–20 October 1982, very heavy rain fell in the Jùcar basin upstream from the Tous Dam. The heaviest rain was recorded in the Cofrentes area, about 25 km northwest of Tous Dam with a total greater than 550 mm and 285 mm falling in only 3 hours. The estimated inflow was 5,000 m^3/s requiring the spillway gates to be opened. Unfortunately, the electrical grid was out of order due to the weather conditions and emergency generators could not be started. Efforts to raise the gates manually were fruitless. The overtopping started at 17:00 with water breaching 1.10 m over the main crest about at 19:15 p.m. So, about 16 hours after trying to open the flood gates, the dam was overtopped, and it washed out within 1 hour by erosion of the central rock-fill. After such an extraordinary flood, in the downstream basin 8 people lost their lives and about 100,000 people had to be evacuated. The damages were estimated to reach $400 million, even if part of these damages were likely to be caused by the floods before the arrival of the break wave (Figure 2). A new Tous Dam was built on the same site and part of the clayey core material, which had shown a relatively high resistance to water flow, was reused for constructing the new dam.

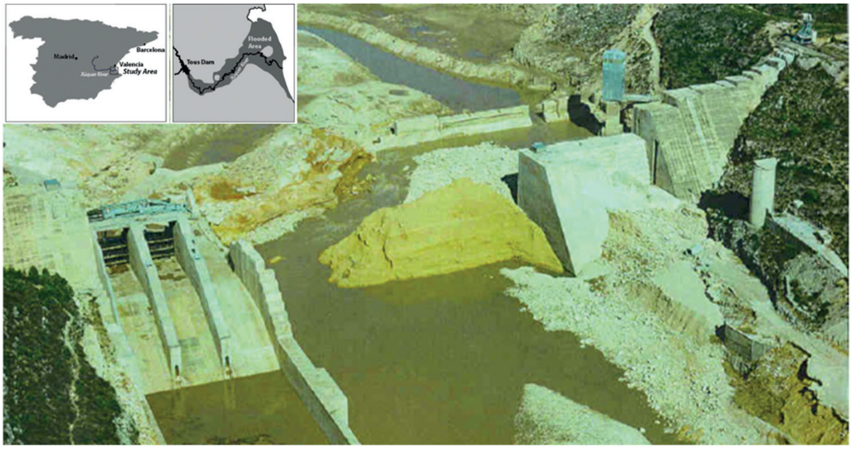

Figure 2. Tous Dam near Valencia, Spain after failure. Note the concrete abutments on both sides and washed-out clay core (yellow material) in the centre [5]

Case Study – Seepage piping failure

Teton Dam, Idaho, USA. Teton Dam, a 93-m-high earthfill dam across the Teton River in Madison County, southeast Idaho, failed completely and released the contents of its reservoir at 11:57 a.m. on 5 June 1976 [3]. Failure was initiated by a large leak near the right (northwest) abutment of the dam, about 40 metres below the crest. The dam, designed by the U.S. Bureau of Reclamation, failed just as it was being completed and filled for the first time. Eyewitnesses noticed the first major leak between 7:30 and 8:00 a.m. 5 June, although two days earlier engineers at the dam observed small springs in the right abutment downstream from the toe of the dam. The main leak was flowing about 0.5–0.8 m^3/s from the rock in the right abutment near the toe of the dam and above the abutment-embankment contact. The flow increased to 1–1.4 m^3/s by 9 a.m. At about the same time, 0.05 m^3/s seepage issued from the rock in the right abutment, approximately 40 metres below the crest of the dam at the abutment-embankment contact.

Between 9:30 and 10 a.m., a wet spot developed on the downstream face of the dam, 5–6 m out from the right abutment at about the same elevation as the seepage coming from the right abutment rock. This wet spot developed rapidly into seepage, and material soon began to slough, and erosion proceeded back into the dam embankment. The water quantity increased continually as the hole grew. Efforts to fill the increasing hole in the embankment were futile during the following 2 to 2 1/2-hour period until failure. The sheriff of Fremont County (St. Anthony, Idaho) said that his office was officially warned of the pending collapse of the dam at 10:43 a.m. on 5 June. The sheriff of Madison County, Rexburg, Idaho, was not notified until 10:50 a.m. on 5 June. He said that he did not immediately accept the warning as valid but concluded that while the matter was not too serious, he should begin telephoning people he knew who lived in the potential flood path.

The dam breached at 11:57 a.m. when the crest of the embankment fell into the enlarging hole and a wall of water surged through the opening. By 8 p.m. the flow of water through the breach had nearly stabilised. Downstream the channel was filled at least to a depth of 9 m for a long distance. About 40% of the dam embankment was lost, and the powerhouse and warehouse structure were submerged completely in debris.

Figure 3. Teton Dam showing progressive piping up to breach [24]

Case Study – Seepage along outlet works

Lawn Lake Dam, Colorado, USA. The dam was in Rocky Mountain National Park upstream of Estes Park, Colorado. It was an embankment dam constructed in 1903 and owned by an irrigation company. It fell within the National Park boundary when the Park was established in 1915. The reservoir was at almost 3,350 m elevation and the dam enlarged a natural glacially formed lake. The dam was raised in 1931 to 7.5 m high and stored a maximum of 1.5 million cubic metres of water [13]. A 1-m diameter, riveted steel outlet pipe was used for releases. A direct-buried gate valve was in this pipe directly under the crest of the dam. The dam was assigned a "moderate" downstream hazard potential. Due to its remote location with challenging access, inspections of the facility were relatively infrequent. Several issues were identified at the dam documented in inspection reports in 1951, 1975, 1977 and 1978.

Between 5:00 and 6:00 a.m. on 15 July 1982, the dam failed suddenly, releasing 1.2 million cubic metres. There was no warning (Figure 4a). The peak flow was approximately 550 m^3/s. The flood wave changed as it went downstream due to the changing topography and the presence of a downstream dam. From the dam, the flood charged down the steep channel of Roaring River. It eroded areas up to 15 m deep. After dropping 760 vertical metres over 7 km, the flood poured out into Horseshoe Park – a relatively flat basin. There it dropped its load of boulders and debris and created an alluvial fan of over 16 hectares. The flood went out the east end of Horseshoe Park, filled and then overtopped a 5-m-high concrete dam called Cascade Dam. The maximum overtopping was 1.2 metres. After 17 minutes of overtopping, Cascade Dam gave way and a new flood surge of 450 m^3/s poured through the breach. In the town of Estes Park, debris-laden, muddy water up to 1.5 m deep (170 m^3/s) poured through the business district. It damaged 177 businesses (over 90% of the businesses). Damages totalled $31 million and a total of three lives were lost. The State Engineer performed an investigation and issued a report 8 months following the failure. The report concluded that "…the failure occurred due to leakage under high pressure from the leaded connection of the outlet pipe and valve, causing progressive piping of the dam embankment in the vicinity of the outlet pipe during periods of high reservoir levels and gate closure and sudden collapse of the embankment allowing rapid evacuation of the reservoir".

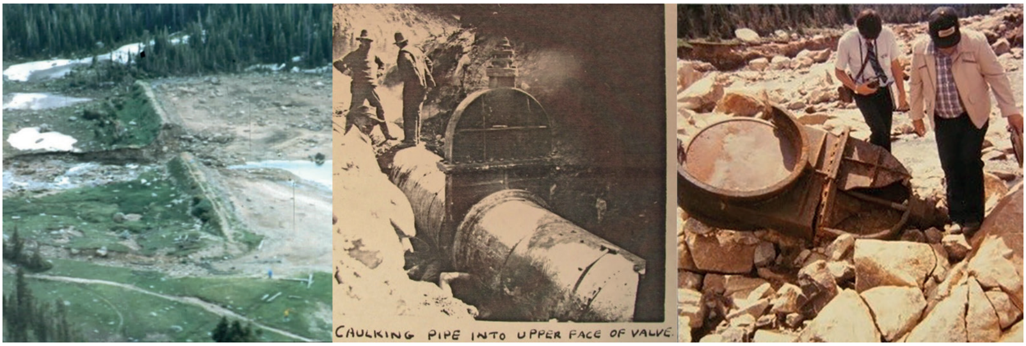

(a) *(b)* *(c)*

Figure 4. Lawn lake a) embankment after failure; b) gate valve improperly installed; c) recovered gate valve 70 m downstream [14]

Case Study – Slope stability

San Luis Dam, California, USA. The 76-m-high San Luis Dam, about 140 km southeast of San Francisco, California, stores water on the California Aqueduct System. These photos (Figure 5a) show a slide that occurred in the upstream slope of the dam in September 1981 [2], as water was being withdrawn from the reservoir. The slide extended for about 330 metres along the embankment. At the north end, near the inlet-outlet structure visible in this photo, the scarp at the top of the slide was about 9 metres high. At the bottom of the slope the toe of the slide moved horizontally about 9 metres out into the reservoir. The head scarp and toe bulge are more clearly visible in Figure 5b. Temporary roads have been cut into the slope to provide access for drill rigs which were used to retrieve samples for testing and to install "slope indicators" that measure movements underground.

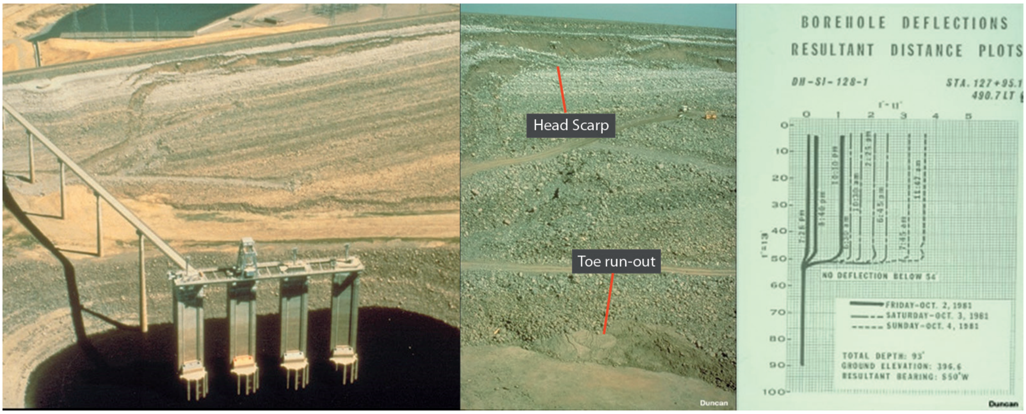

(a) *(b)* *(c)*

Figure 5. San Luis Dam showing a) upstream slope failure due to rapid drawdown; b) closer view of head scarp; c) slope indicator output showing the sharp deflections where failure surface runs [2]

The plot of data from a slope indicator (Figure 5c) shows a distinct rupture surface at a depth of 52 feet (16 m). At this depth the soil is highly plastic clay called "slope wash", on which the embankment was constructed. In its dry condition the slope wash was nearly as hard as a brick. However, the tests showed that the slope wash became very weak when wetted contributing to the principal cause of the slide.

Case Study – Liquefaction

Lower San Fernando Dam, California, USA. The upstream slope of the Lower San Fernando Dam, in California, failed due to liquefaction during the 1971 San Fernando earthquake. The dam was constructed by "hydraulic filling", which involves mixing the fill soil with a large amount of water, transporting it to the dam site by pipeline, depositing the soil and water on the embankment in stages, and allowing the excess water to drain away. The fill that remains is loose and is subject to liquefaction as the result of earthquake shaking. About 1 m of freeboard remained after the upstream shell slid into the reservoir (Figure 6a). The paved crest of the dam can be seen descending into the water at the top of this photo. Fortunately, the intake structure was undergoing repairs, requiring a reduced level in the reservoir. The slide in the upstream shell is shown in Figure 6b with the reservoir emptied. The paved road surface identifies the former crest of the dam. With every case study comes new information and insight, enabling engineers to avoid mistakes and produce better and safer designs. The interested reader is invited to visit the website http://damsafety.org/ and http://damfailures.org/.

(a) *(b)*

Figure 6. Lower San Fernando Dam, upstream face showing liquefaction slide due to earthquake (M 7.1) shaking, a) immediately following the earthquake; b) after the reservoir was drawn down [17]

Considering failure modes in design

Part of the design process is to envision the types of failure scenarios that may occur. Figure 7 illustrates some scenarios that may occur and require consideration.

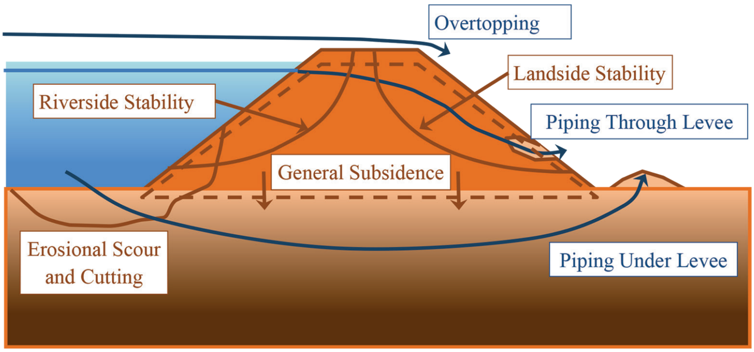

Figure 7. Some failure modes for levees and dams (compiled by the author)

While overtopping is perhaps more in the area of flow prediction and reservoir sizing, there are geotechnical aspects as well. Some embankments are meant to be overtopped as emergency spillway. The critical soil property is then resistance to erosion so that the overtopping water will not cut a deep channel through the embankment. Other conditions where erosion resistance is important occur when flood waters try to scour away the toe of a riverside slope. This may be due to wave or current action, or both. Scouring may occur under (concrete) foundations of hydraulic control structures as well.

One of the most critical tasks in levee design is concerned with water seepage through and under the levee during flood events. Seepage under or through the levee may go undetected until it is too late. It is also complicated by the fact that soil hydraulic conductivity can vary by 12 orders of magnitude. Such a wide variation means that thin, undetected soil layers may control where and how much seepage occurs.

Stability of the levee is controlled by the strength of the embankment materials and the soils beneath it [16]. Unfortunately, embankment materials that perform well at blocking seepage are not very strong. Conversely, soils that provide good slope stability are poor seepage barriers. This is the primary reason for zoned embankment dam design. Each zone in the dam performs a different function, and by working together, they achieve the necessary stability and seepage blocking requirements.

General subsidence (settlement) may occur when the embankment soils, or soft foundation soils, compress or consolidate over time. This leads to reduced crest height in the dam or levee. Differential settlement may cause cracking in the embankment or functional loss of control gates or other mechanical features that require precise dimensional tolerances.

Connecting failure modes, methods of analysis, required data

Based on the possible failure scenarios above, one must consider the methods to evaluate their likelihood as well as the data necessary to perform meaningful analyses. Table 1 shows the pertinent soil properties, laboratory and field tests, and common analyses required in order to assess the level of safety for a levee.

This table is by no means exhaustive but is meant to demonstrate the relationships between different possible failure scenarios and the methods to evaluate them. Not shown in the table are the field and laboratory testing that is performed to better define the extents of different soil layers throughout the site as well as other index and classification tests used to confirm that soil in one location is indeed the same (or not) as soil in another location.

Table 1. Failure modes, soil properties, tests and analyses to evaluate the possibility of failure (compiled by the author)

Failure Mode	Required Soil Properties	Field Tests	Laboratory Tests	Analysis
Overtopping Toe Erosion and Scour	Erodability Dispersivity Soil strength	Jet Erosion	Erosion Function Apparatus Clay Dispersion	SRICOS HEC-18 EUROSEM Infinite slope analysis
Seepage and Piping	Hydraulic Conductivity SWCC (unsat.) Dispersivity	Well tests CPT injection Tensiometers	Constant Head Constant Flux Pressure Plate Clay Dispersion	Groundwater Flow, Unsaturated Flow
Slope Stability	Soil Strength (cohesion, phi)	CPT Dilatometer Sample Boring	Triaxial Strength Direct/Simple Shear Proctor Compaction	Slope Stability FEM Displacements
Embankment Subsidence	Soil Compressibility	CPT Dilatometer Sample Borings	Consolidation Creep Proctor Compaction	Hand Computation of Settlement FEM Displacements

Note: Classification, Grain Size, Atterberg Limits and other index tests would be part of all of these assessments

Principal design cross sections

Based on the concept that soils can rarely perform both seepage and stability functions well, typical cross sections for dams and levees have evolved to zoned earth dams. A purely homogeneous embankment will allow seepage water to exit the landside face and create piping and stability problems there. So, even rudimentary dams have a drainage system to direct seepage out of the embankment in a controlled manner (Figure 8a, b). Dams with a core material (typically clay) greatly reduce seepage volumes but require transition zones to help keep the core in place and provide more dependable stability.

Additional challenges with flood levees

Some obvious problems occur when engineers try to build a levee system alongside a meandering river such as the Mississippi River in the U.S. or parts of the Danube and Tisza in Hungary [1] [10] [22]. While the terrain is flat, the underlying Holocene geology is very heterogeneous and complex. A typical section may look like the illustration in Figure 9 where old river channels and flood features underlie the present river system.

This also means it underlies the levee system, as well and will connect seepage sources to different places behind the levee, defying any two-dimensional approach. There may be deposits that are moderately deep beneath the levee that later reach the surface over 300 m from the levee embankment.

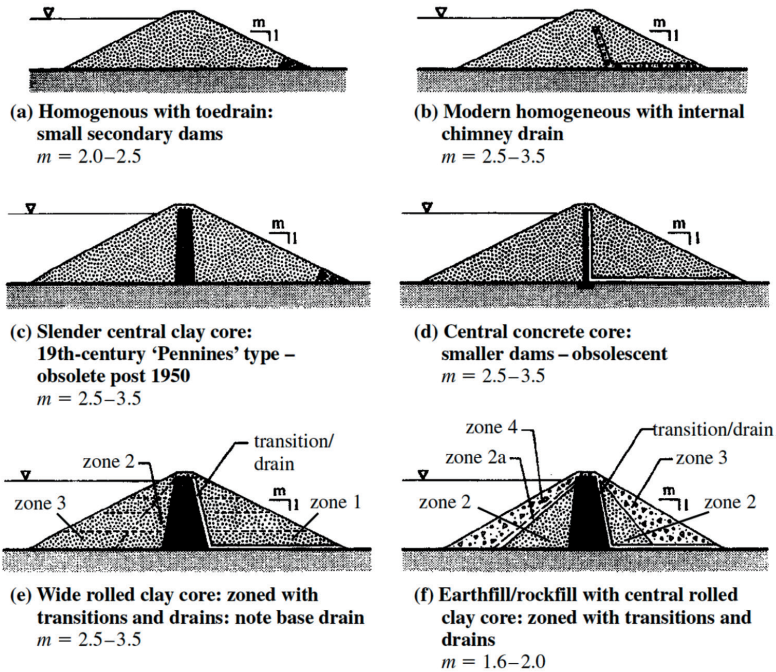

Figure 8. Typical dam or levee cross-sections, simplest (a) to most complex (f) [22]

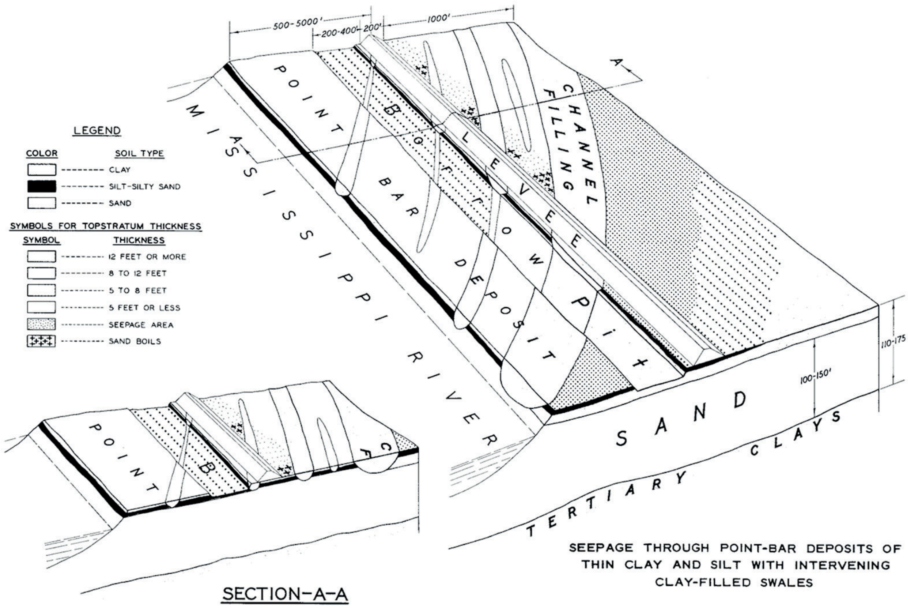

Figure 9. Holocene deposits along meandering river channel [20]

Basic soil mechanics

Description and classification of soils

Soil is defined for engineering purposes as a natural aggregate of mineral grains separable by gentle mechanical means, e.g., agitation in water. Rock in contrast, is a natural aggregate of minerals connected by strong and permanent cohesive bonds. The boundary between soil and rock is to some degree arbitrary, as exemplified by soft or weathered rocks, e.g. weathered limestones and shales, or weakly cemented sandstones. All engineering soils of non-organic origin (i.e. excluding peats, etc.) are formed by rock weathering and degradation processes. These may occur in situ forming residual soils. Alternatively, if the rock particles are removed and deposited elsewhere by natural agents, e.g., glaciation or fluvial action, they will form transported soils. Soft or weathered rocks form part of the range of residual soils. Transportation results in progressive changes in the size and shape of mineral particles and a degree of sorting, with the finest particles being carried furthest.

All engineering soils are particulate in nature, and this is reflected in their behaviour. An important distinction must be drawn between two generic inorganic soil groups which result from different weathering processes [15]. The larger, more regularly shaped mineral particles which make up silts, sands and gravels are formed from the breakdown of relatively stable rocks by purely physical processes, e.g. erosion by water or glacier, or disintegration by freeze–thaw action. Certain rock minerals are chemically less stable, e.g. feldspar, and undergo changes in their mineral form during weathering, ultimately producing colloidal-sized ‘two-dimensional’ clay mineral platelets.

These form clay particles, the high specific surface and hence surface energy of which are manifested in a strong affinity for water and are responsible for the properties which particularly characterise clay soils, i.e. cohesion, plasticity and susceptibility to volume change with variation in water content. Differences in platelet mineralogy mean that clay particles of similar size may behave differently when in contact with water, and hence differ significantly in their engineering characteristics. Soil particles vary in size from over 100 mm (cobbles) down through gravels, sands and silts to clays of less than 0.002 mm size. Naturally occurring soils commonly contain mixtures of particle sizes but are named according to the particle type that controls its general behaviour. Thus, a clay soil is so named because it exhibits the plasticity and cohesion associated with clay-mineral-based particles, but the mineral matrix invariably contains a range of particle sizes, and only a minor proportion of the fine material in the matrix may be clay sized, i.e. < 0.002 mm (2 μm) as shown in Figure 9. One system (Unified Soil Classification System) used for defining and classifying the particle size ranges for soils is provided in Figure 11.

The divisions between the named soil types correspond broadly to significant and identifiable changes in engineering characteristics. Particle size analysis is therefore employed for primary classification, to distinguish between gravels, sands and fine-grained silts and clays [6]. However, particle size analysis is insufficient for the complete classification of fine-grained soils or coarser soils where the matrix includes a proportion of plastic fines, i.e. clays (e.g. Figure 10c–f). Classification by plasticity is then necessary, using limits expressed in terms of percentage water content by mass.

The liquid limit, wL, is the water content defining the change in soil consistency from plastic to liquid; the plastic limit, wP, defines the change-point below which a soil is too dry to exhibit plasticity. The range between wL and wP is plasticity index, IP, with IP = wL – wP. Secondary classification is determined through IP and wL using classification charts.

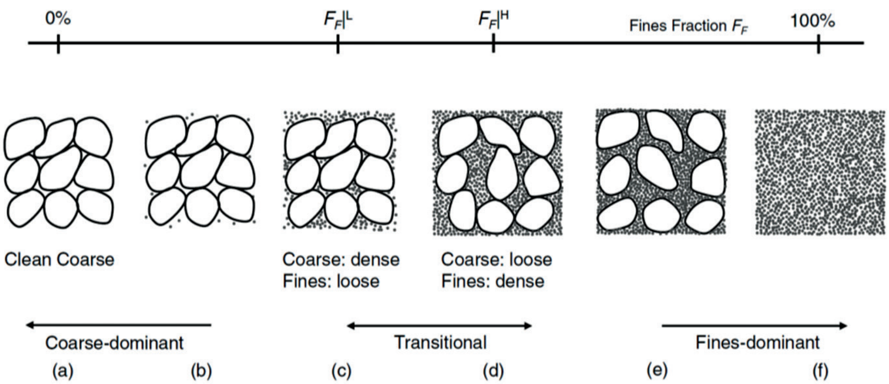

Figure 10. Transition from coarse to fine-grained soil [14]

Note that fine material has dominant effect, even at low weight percentage

The Unified Soil Classification System (Figure 11) divides soils into groups, each of which is denoted by a two-letter symbol. The first letter is the dominant soil constituent, i.e. G, S, M and C for gravels, sands, silts and clays respectively. The second provides descriptive detail based on particle size distribution for coarse soils, e.g. SW = well-graded sand, or on the plasticity of fines.

Criteria for assigning group symbols				**Group Symbol**
Coarse-grained soils More than 50% retained on No. 200 sieve	**Gravels** More than 50% of coarse fraction retained on No. 4 sieve	Clean Gravels	$C_u \geq 4$ and $1 \leq C_c \leq 3$[c]	**GW**
		Less than 5% fines[a]	$C_u < 4$ and/or $1 > Cc > 3$[c]	**GP**
		Gravels with Fines	*PI* < 4 or plots below *"A"* line	**GM**
		More than 12% fines [a,d]	*PI* > 7 and plots on or above *"A"* line	**GC**
	Sands 50% or more of coarse fraction retained on No. 4 sieve	Clean Sands	$Cu \geq 6$ and $1 \leq C_c \leq 3$[c]	**SW**
		Less than 5% fines[b]	$Cu < 6$ and/or $1 > C_c > 3$[c]	**SP**
		Sands with Fines	*PI* < 4 or plots below *"A"* line	**SM**
		More than 12% fines [b,d]	*PI* > 7 and plots on or above *"A"* line	**SC**
Fine-grained soils 50% or more passes No. 200 sieve	**Silts and Clays** Liquid Limit less than 50	Inorganic	*PI* > 7 and plots on or above *"A"* line	**CL**
			Liquid Limit less than 50	**ML**
		Organic	$\frac{\text{Liquid Limit oven dried}}{\text{Liquid Limit not dried}} < 0.75$	**OL**
	Silts and Clays Liquid Limit 50 or more	Inorganic	*PI* > 7 and plots on or above *"A"* line	**CH**
			PI < 4 or plots below *"A"* line	**MH**
		Organic	$\frac{\text{Liquid Limit oven dried}}{\text{Liquid Limit not dried}} < 0.75$	**OH**
Highly Organic Soils	Primarily organic matter, dark in color, and organic odor			**Pt**

(a) Gravels with 5 to 12% fines require dual symbols GW-GM, GW-GC, GP-GM, GP-GC
(b) Sands with 5 to 12% fines require dual symbols SW-SM, SW-SC, SP-SM, SP-SC
(c) $C_u = \frac{D_{60}}{D_{10}} \quad C_c = \frac{(D_{30})^2}{D_{60} \times D_{10}}$
(d) If $4 \leq PI \leq 7$ and plots in hatched area use dual symbol GC-GM or SC-SM
(e) If $4 \leq PI \leq 7$ and plots in hatched area use dual symbol CL-ML

Figure 11. Classification criteria for soils [6]

Normally, sieve analysis for coarse soil; sieve, hydrometer and liquid/plastic limits for fine grained soils are required. Such tests are routinely performed on a daily basis in a laboratory.

Hydraulic conductivity of soils

One of the key soil performance properties for flood control is hydraulic conductivity. It is a measure of how easily water travels through soil. By simply observing different soils, one may appreciate the vast differences between gravels and clays. The degree of conductivity is related to the size and connectivity of pore spaces within soils. Gravel, with larger pores that are well connected exhibits high conductivity while clay particles often have pores only microns in size have very low conductivity. The numerical property is generally based on the assumption that water flow through soil is independent of the degree of pressure (gradient) being used to push it through. Measuring this value is often done in the field through pumping tests and borehole tests and in the laboratory by controlled head or controlled flow tests. It is easier to discuss measurement using a simple laboratory test called the constant head test, shown in Figure 12.

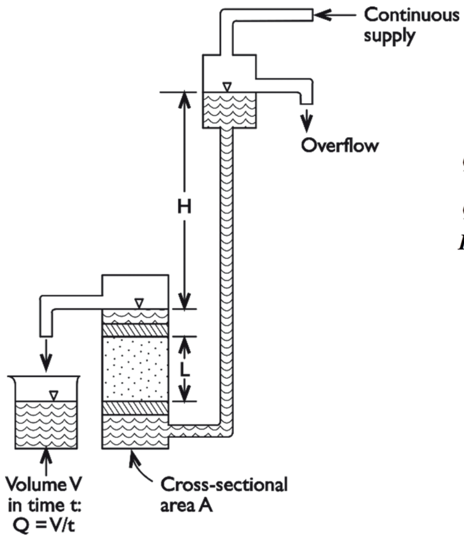

Darcy's Law States

$$Q = kiA = k\frac{H}{L}A \quad \text{or} \quad k = Q\frac{L}{HA}$$

Q = measured as $V\,/\,t$ (m^3/sec)

H = measured as difference in height shown (m)

L = length of specimen (m)

k = hydraulic conductivity (m/sec)

Set H = 30 cm, Sample L = 10 cm, A = 12 cm^2

Measure V = 200 cm^3, t = 120 sec

$$k = \frac{200}{120}\frac{10}{30\times 12}\left(\frac{cm^3}{sec}\frac{cm}{cm\ cm^2}\right) = 0.046\left(\frac{cm}{sec}\right)$$

$$k = 4.6\times 10^{-4}\left(m\,/\,sec\right)$$

Figure 12. Darcy's Law applied to laboratory constant head test [14]

The example calculation is a reasonable set of numbers for a laboratory test. There are many correlations between soil type and hydraulic conductivity. Table 2 lists one such set. Note the very wide range of values possible and the influence of the clay fraction in sands and gravels (GC, SC). Maintaining some level of quality control in the selection of embankment materials and treatment of foundation soils is very important because even a small variation in soil mixture can change conductivity by 1000x. One might also appreciate the dangers of having a thin layer of dissimilar material that would block (low k) or pipe (high k) seepage through the levee. Since a laboratory specimen is indeed small compared to the site, field tests are often performed to verify conductivity values determined in the laboratory. Another useful function of laboratory tests is to evaluate how soil improvements (compaction, injections, additives) will affect conductivity. Hydraulic conductivity will play a key role in determining the influence of seepage through and under the embankment. This will be addressed in a later section on seepage.

Table 2. Approximate hydraulic conductivity values for different soil types [14]

Description	USCS	min. (m/s)	max. (m/s)
Well graded gravel	GW	5.00E-04	5.00E-02
Poorly graded gravel	GP	5.00E-04	5.00E-02
Silty-sandy gravels	GM	5.00E-08	5.00E-06
Clayey gravels	GC	5.00E-09	5.00E-06
Well graded sands	SW	1.00E-08	1.00E-06
Poorly graded sands	SP	2.55E-05	5.35E-04
Silty sands	SM	1.00E-08	5.00E-06
Clayey sands	SC	5.50E-09	5.50E-06
Inorganic silts	ML	5.00E-09	1.00E-06
Inorganic clays	CL	5.00E-10	5.00E-08
Organic silts	OL	5.00E-09	1.00E-07
Silts of high plasticity	MH	1.00E-10	5.00E-08
Clays of high plasticity	CH	1.00E-10	1.00E-07
Compacted silt	(ML-MH)	7.00E-10	7.00E-08
Compacted clay	(CL-CH)	–	1.00E-09
Organic highly plastic clays	OH	5.00E-10	1.00E-07
Peat/highly organic soils	Pt	–	–

Soil strength, compressibility and stability

In order to remain stable, a dam or levee must have material that resists sliding and does not consolidate or compress too much under its own weight. Sliding stability is related to shear strength of soils while compressibility is a function of the bulk stiffness of the soil. The most common tests to determine shear strength are triaxial tests. A cylindrical specimen is subjected to confining pressure (simulating burial at a particular depth) then vertical load is applied until failure. This test is often repeated on several similar samples using progressively higher confining pressure. Once this is completed, an estimate of strength properties, based on cohesion (c) and friction angle (ϕ), can be deduced (Figure 13). Typical values for strength for different soils are shown in Table 3.

Table 3. Typical strength values for soils [6]

Clays–Description	Strength	Sands–Description		Cohesion–Friction
Hard soil	Su > 150 kPa	Compact Sands		35°–45°
Stiff soil	Su = 75–150 kPa	Loose Sands		30°–35°
Firm soil	Su = 40–75 kPa	Overconsolidated Clay		
Soft soil	Su = 20–40 kPa	Critical State	c' = 0	ϕ' = 18°–25°
Very soft soil	Su < 20 kPa	Peak State		c' = 10–25 kPa ϕ' = 20°–28°
		Residual		c' = 0–5 kPa ϕ' = 8°–15°

Cohesion is more likely to be associated with clayey soils, while friction angle comes from sandy soils. Of course, a soil can have both, and often does. If the soil on-site is saturated (almost always with dams and levees), then soil testing should be performed under effective stress conditions. Effective stress includes the effects of pore water pressure within the soil, usually denoted as:

$$\begin{aligned} \boldsymbol{\sigma'} &= \boldsymbol{\sigma} - \boldsymbol{u} \\ \boldsymbol{\sigma'} &= \text{effective stress} \\ \boldsymbol{\sigma} &= \text{total stress (soil pressure and water pressure)} \\ \boldsymbol{u} &= \text{pore pressure (pressure of water within soil)} \end{aligned} \quad (1.1)$$

Pore pressures can increase or decrease during the shearing process and therefore the effective stress may change as well. Once effective stresses are accounted for (most software will do this automatically), the strength properties are developed in exactly the same way. Pore pressures (if there are any developed) are subtracted from the confining stress, effectively moving each failure circle (σ_{3a}-σ_{1a}, σ_{3b}-σ_{1b}, σ_{3c}-σ_{1c}) to the left on the graph a distance equal to the pore pressure generated during the test.

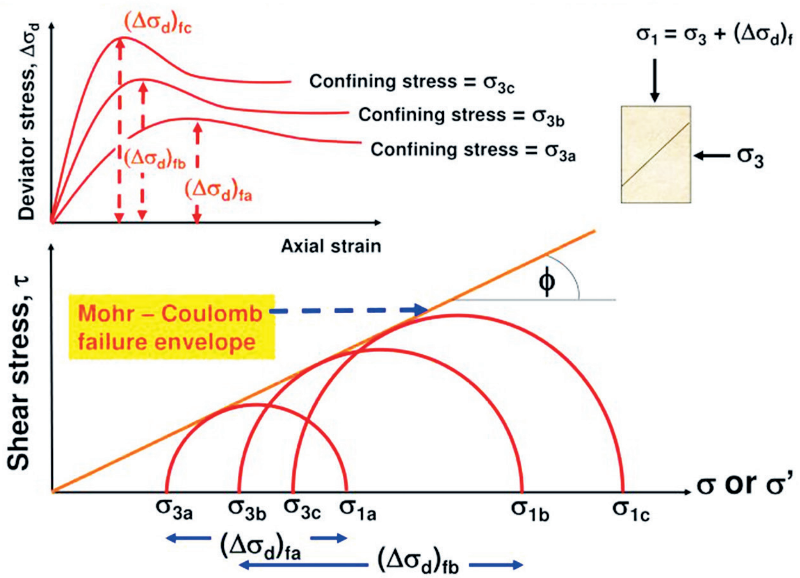

Figure 13. Series of three triaxial tests at increasing confining stress [6]

Note differences in stress-strain curves. For this soil, c = 0 and $\phi = 25°$

Consolidation is a process where firm or soft saturated clays are loaded from above and attempt to squeeze out pore water. Since clays have a low hydraulic conductivity, this process is slow, perhaps taking years to complete. As the pore water migrates out of the clay, its pores become smaller, causing settlement. Engineers need to know how much consolidation settlement it is likely, and how long will take to complete. Both answers come from a consolidation test in the laboratory. A typical test consists of several stages of loading with each stage requiring about 24 hours to complete (Figure 14a). As one stage is completed, load is doubled and the next stage started. The specimen may be unloaded as well to determine rebound behaviour. When the stages are completed, a summary plot is generated and the oedometer modulus E_{oed} can be determined (Figure 14b). Time to complete 50% or 90% of consolidation is also determined. The oedometer modulus can be applied to the field soil profile to determine how much settlement may occur. The time to complete consolidation is scaled from laboratory conditions to field conditions; depending mainly on the distance required for the pore water to reach a drainage layer.

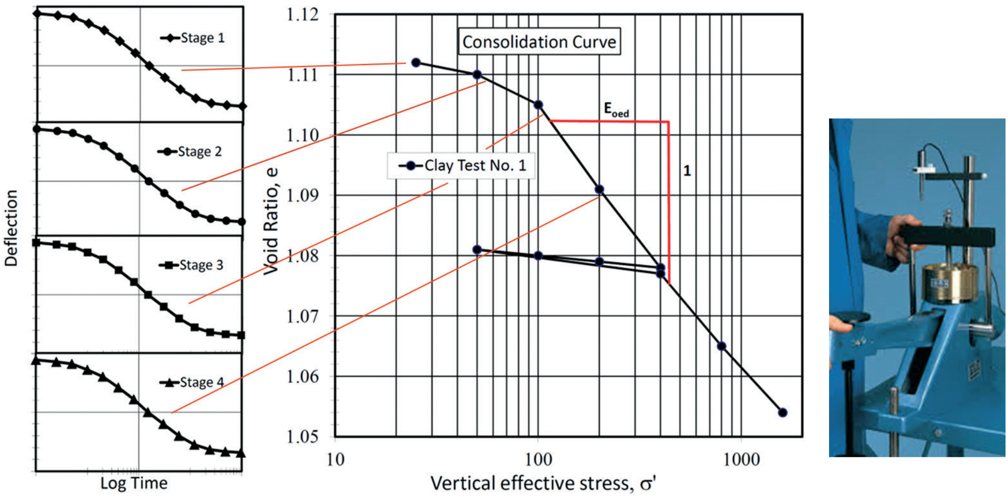

(a) *(b)* *(c)*

Figure 14. One-dimensional consolidation testing to determine (a) rate of settlement; (b) magnitude of settlement; (c) device [6]

Methods of seepage analysis

When evaluating a levee's ability to resist seepage breakthrough, the conceptual model mentioned earlier shows the various combinations of problems that may occur (Figure 7). Note that these effects often interact with each other to weaken stability or provide a more ready pathway for ground water to flow. Seepage is not necessarily bad; however, uncontrolled seepage can lead to severe problems. In this section, the main ideas about determining the quantity and direction of seepage through a dam or levee are presented.

Flow nets and flow paths

The simplest way to estimate where seepage will travel is to construct a flow net. It is a graphical method for deducing the path water will follow as well as water pressure (head, pore pressure) and gradient ($i = dh/dl$ = change in head/distance travelled). All of these quantities are important for the proper functioning of a dam or levee.

A flow net consists of two families of lines: equipotential lines and flow lines. Equipotential lines represent locations where water head (pressure + elevation head) are equal. Figure 15 shows them with red lines. Flow lines represent the path seepage water takes from the source (river, reservoir, lake) to the exit point (hopefully a drain or outflow). Figure 15 shows them with green lines.

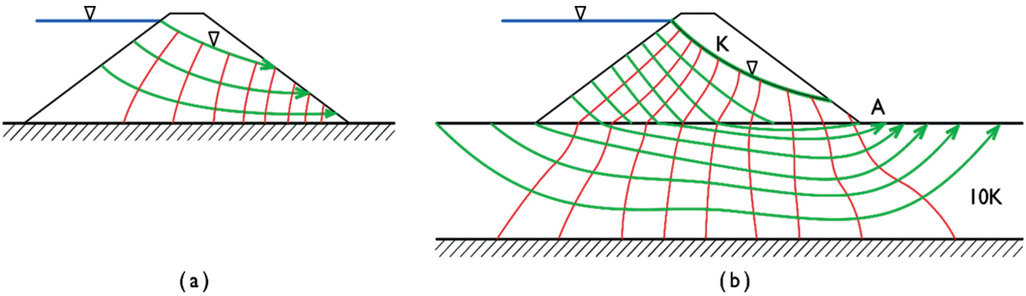

Figure 15. Flow nets drawn through an earth dam with (a) impervious foundation; (b) pervious foundation (compiled by the author)

The embankment in Figure 15a is resting on an impervious foundation; therefore, no water is seeping below it. The configuration in Figure 15b includes foundation soils with approximately 10 times higher hydraulic conductivity. Important design factors to note include the exit point on the downstream slope of Figure 15a and somewhat reduced exit on Figure 15b. Both would be unacceptable as designs. Exit gradient can be estimated if the head loss for each equipotential line (Δh) is known as well as the physical distance between the lines (Δl). Gradient is then:

$$\boldsymbol{i} = \frac{\boldsymbol{\Delta h}}{\boldsymbol{\Delta l}} \quad (1.2)$$

As the flow line is directed upward near point A in Figure 15b, it will tend to lift the soil up and out of place. This occurs when the gradient reaches approximately i = 0.85. Exit gradients of this magnitude may create exit seeps along the downstream edge of the levee or dam [14]. Drawing flow nets for conditions that are even moderately complex requires a great deal of practice and technique beyond this course. However, most seepage software programs produce equipotential lines quite readily, and will produce flow lines as part of its post-processing activity.

Seepage analysis software

There are a great number of software programs that will analyse seepage below and through dams and levees. The most common approach is a two-dimensional finite element method. Finite elements are a way to approximate non-linear field behaviour (in this case, seepage through soil) by dividing the problem domain into a finite number of elements where each has a behaviour that can be described by a simple (e.g. linear or second-order equation). Each element may have its own material properties, such as hydraulic conductivity and are connected by sharing common nodes with neighbouring elements. So, instead of defining a problem with an intractable mathematical formulation, finite elements break the problem into smaller, simpler pieces. For seepage problems, the result is a physical problem where the soil transmissivity matrix (hydraulic conductivity and element geometry combined) is first assembled. Boundary conditions are then applied, typically as constant head boundaries (such as a reservoir or flood level) then the unknown values of the total head are computed for every nodal point in the domain. The price of simplification is that many nodes and elements are required to generate an accurate model of the physical problem. Models with over 5,000 nodes (and unknowns) are common. As complexity increases, the software may have to compute more than just a steady-state solution. Flood waves are time-dependent, as are scenarios for reservoir filling and emptying. This requires a multi time step approach using unsaturated hydraulic conductivity values. The problem must then be solved for every time step. Additional boundary conditions may be needed such a rainfall, pumping or other transient events. If the problem requires a three-dimensional model, the numerical solutions become very time consuming with perhaps 50–100,000 nodes and equations.

Shown below are just two examples of a 2D problem with a dam and reservoir. The boundary conditions are 8-m total head elevation at the reservoir and 0-m total head elevation at the downstream toe. Figure 16 shows the flow regime for a homogeneous dam. There is only one type of soil throughout. The contour lines of equal total head are labelled for every 0.5 m. Note the very high exit velocity arrows near the downstream toe. This would indicate that the water would carry away the downstream slope until it failed. Flow lines move evenly through the dam from the reservoir to the downstream side. The flow net produced is very similar to Figures 15a, b. This particular software also models unsaturated flow, so there is no free (phreatic) surface through the dam. It could be drawn by connecting points on total head contours at their corresponding elevation. A more engineered approach is shown in Figure 17 where there is a centre core of lower conductivity soil (clay) and a toe drain of higher conductivity soil (gravel). Note that many of the total head contours are inside the clay core. That is because the core dissipates seepage energy, leaving much less energy toward the downstream toe. The toe drain draws flow to it, which is good, because the gravel in the toe drain is much less likely to be lifted out and away from the downstream slope. The total flow of water through this dam is about one-tenth of that shown in Figure 16.

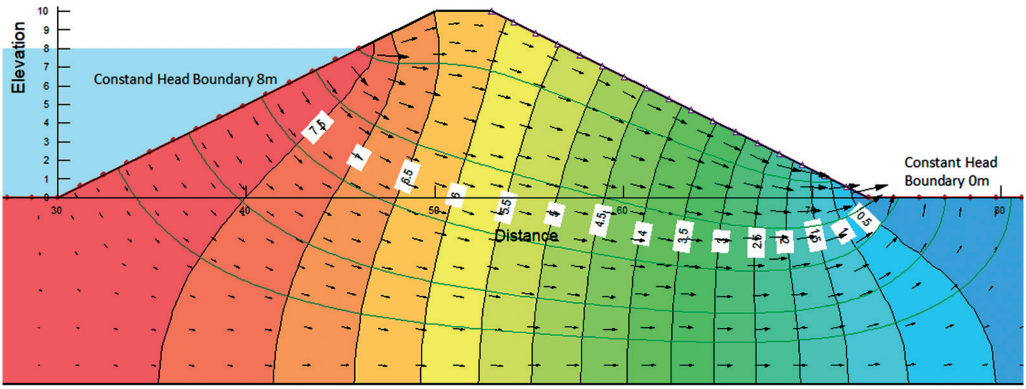

Figure 16. Flow through homogeneous dam (compiled by the author based on [8])
Note the very strong exit velocity at the downstream toe

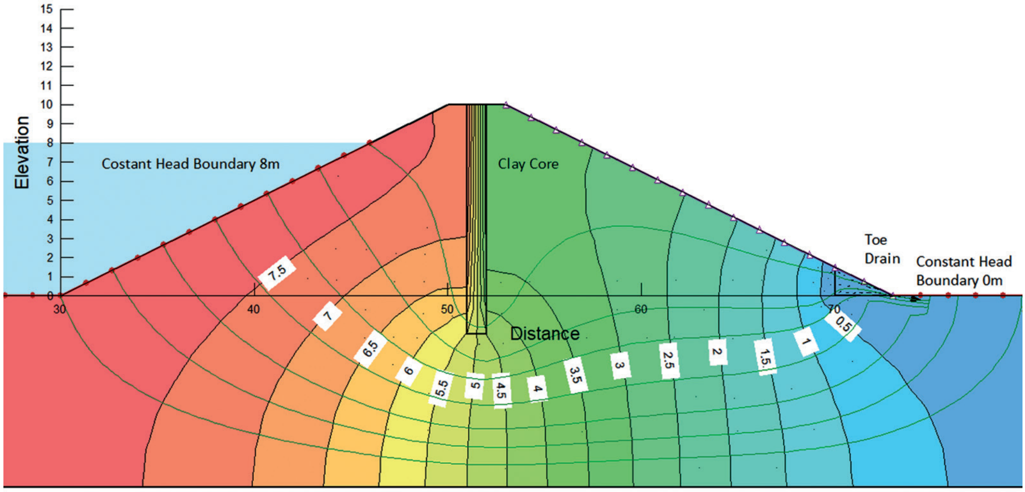

Figure 17. Seepage through a dam with a clay core and gravel toe drain (compiled by the author based on [8])

Special seepage problems with flood levees

Assessing seepage problems in levees is more difficult than in dams. Levees can be many kilometres long and are required to hold back water until a flood event occurs. It is difficult to determine how well a levee will perform until the flood wave arrives; not the best time to find out if the levee is performing properly. Since levee systems are so extensive, many embankments are nearly homogenous. Others may have an upstream blanket and some sort of toe drain system, but this is not always the case. One of the most persistent problems in levee performance is the generation of exit sand boils (Figure 17). They occur regularly during floods and are very difficult to predict and remediate [1] [18].

Since the analysis and evaluation of levees are limited in complexity, several methods have been developed to evaluate the levee embankment and foundation soils as an entire unit. Some methods apply only to specific boundary conditions or when the hydraulic conductivity of the levee is very small (1/1000) compared to the foundation soils. Other assumptions may include homogeneity of the foundation soils, or the levee embankment, or simple layered systems.

Assumptions concerning anisotropy are important as well. All methods can be used to obtain seepage quantities but may not give seepage gradients, pressures, or forces. Table 3 provides guidance about the information that can be obtained from each procedure.

Figure 18. Sand boil created by high exit gradient (sandbags have been piled around the opening to increase the downstream head and reduce the gradient) [10]

Table 4. Methods of analysis and what they compute (Comp.) or estimate (Est.) (compiled by the author)

Method	Gradients	Pressures	Seepage Quantity
Flow Net	Comp.	Comp.	Comp.
Embankment Phreatic Line	Comp.	Est.	Comp.
Unconfined Aquifer (Dupuit's assumption)	Est.	Est.	Comp.
Confined Aquifer of finite length and uniform thickness	Est.	Est.	Comp.
Blanket-Aquifer (Continuous and Discontinuous)	Est.	Comp.	Comp.
Finite Element Models	Comp.	Comp.	Comp.

Analysis by Hungarian designers is very similar to that shown above. In section 7 of the Hungarian floodwater defence handbook, the categories of models are identical to the phreatic line discussed by Casagrande and by Kozeny; and applied to several configurations. Additional configurations were analysed using the Blanket-Aquifer approach developed by [1] and extensively modified by others as it was incorporated into the design procedures for the U.S. Army Corps of Engineers [20] [22] [23] for use in the Mississippi River system. Other methods of analysis used in Hungary were based on modifications to work by Dachler, Davidenkoff and Pavlovsky [25].

Through berm analyses

The through berm (embankment) analyses generally assume flow in the foundation soils. This is a reasonable assumption if the foundation soils have conductivities 1/100–1/1000 times that of the levee berm. Some analyses consider the berm and foundation soils to have nearly the same conductivity. Most of these analyses focus on the point of exit of seepage on the landside of the berm. If the exit point is too high and the seepage velocity too great, internal piping will take place followed by a land-side collapse.

Under-berm analyses

Flow of seepage under the levee receives more attention because it is more difficult to detect and prevent. Often, some form of blanket layer is assumed to exist that restricts horizontal flow near the surface of the foundation soils. However, it will not restrict vertical flow into lower, more permeable layers, nor is it able to stop the upward movement of water on the landside. This gives rise to sand boils or blanket heave where seepage gradients are high enough to erode soil away from the exit point. The under-berm analyses generally assume no flow in the berm soils, vertical flow in the blanket soils and horizontal flow in the foundation soils. Many simplifying assumptions are made in these analyses to compute overall flow and exit gradient. Typical general blanket flow geometry is shown in Figure 19.

The figure is taken from [11], perhaps the most comprehensive reference on blanket theory today. Shown in the figure are three foundation zones: 1. Inflow on riverside; 2. Horizontal flow below levee; 3. Outflow on landside. Also shown are the pressure-head line within the foundation layer (there is no flow through the levee embankment) and either side of the levee, as well as critical head values used in calculating flows and gradients. On the extreme right and left are shown assumptions of flow or no-flow conditions which will affect the derivation of formulae and final results. An impermeable layer at depth simplifies assumptions of continuity. The authors use a coordinate system with the origin at the centre of the levee which allows for a more compact solution.

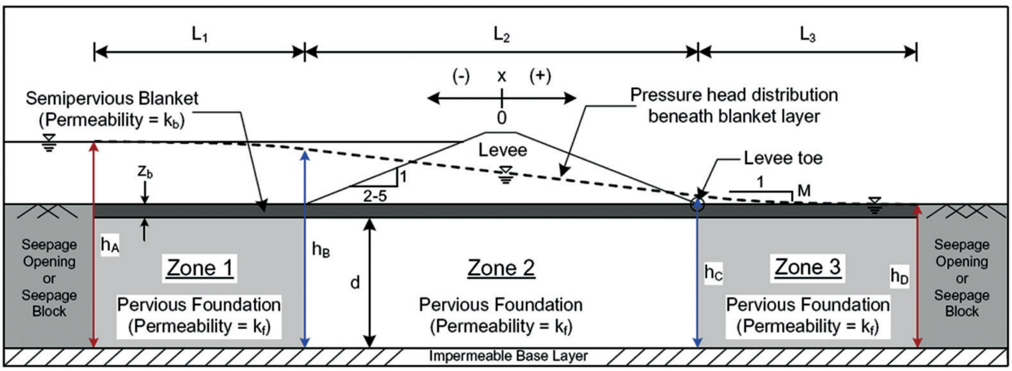

Figure 19. Typical blanket configuration [11]

Using the configuration shown above reduces the seepage assessment to families of equations that can be solved on a spreadsheet. This greatly simplifies analysis and allows the engineer to evaluate performance of a wide variety of geometric and conductivity values.

Levee field performance in the U.S.

Most levees in the U.S. are under the supervision of the U.S. Army Corps of Engineers (USACE) with a large percentage associated with the Mississippi/Missouri River system. Seepage performance of flood levees have been evaluated and analysed for over 70 years on the river system. Some of the observations are listed in the following paragraphs.

Lower Mississippi River. [19,20,21] reported the analysis of piezometer data obtained at 15 piezometer sites during the 1950 high water and selected sites at other times. Conclusions pertinent to this study included the following:

a) Sand boil occurrence. The locations of sand boils were highly correlated with local geologic conditions. In point bar areas, most sand boils occurred in ridges adjacent to swales. Sand boils also tended to occur between levees and parallel clay-filled plugs and in landside ditches.

b) Sand boil gradients. Where sand boils occurred, measured gradients were in the range 0.5 to 0.8, often about 0.65, and generally lower than the 0.85 value used in the analysis procedure. Two influencing factors were suggested: old boils may be reactivated at relatively low pressures, and the pressure relief resulting from the boil may lower piezometer readings in the area.

c) Entrance and exit distance. Both the entrance (L1) and exit (L3) distances varied with river stage. In certain cases, a reduction in the entrance distance with river stage was attributed to scour in riverside borrow pits. It was observed that calculated entrance and exit distances were quite variable, and that a 0.015-m reading error in each of two piezometers could result in substantial error in calculating these distances.

d) Permeability ratios. Ratios of the substratum horizontal permeability to the landside top stratum vertical permeability, back figured from the entrance and exit distances, were typically in the range 100 to 2,000.

e) Permeability. Apparent top blanket permeability decreased as top blanket thickness increased as a result of sealing defects, such as root holes and cracks. Also, the permeability of the landside blanket was 2 to 10 times that of the riverside blanket because of downward flow sealing defects and upward flow opening defects.

Mid-Mississippi River. [21] and [25] reviewed the performance of the Alton-to-Gale (Illinois) levee system along the middle Mississippi River during the record flood of 1973. The review was based on approximately 20,000 piezometer readings obtained from approximately 1,000 piezometers along 384 km of levee.

a) Characterisation by two soil layers. Critical reaches with respect to under seepage had a thick (6- to 15-m) layer of sandy silt or silty sand beneath the top blanket and above more pervious sands. In the present analysis and design procedure, this “intermediate” stratum must be mathematically transformed and combined with either the top blanket or substratum. When wells were designed and installed, the intermediate stratum was blanked off as the materials were too fine for the standard filter and screen. During floods, such wells may flow profusely yet piezometers at the base of the top blanket indicate excessive residual heads. This phenomenon occurs because the horizontal permeability of the intermediate stratum is greater than the vertical permeability of the substratum, causing seepage in the intermediate stratum to be more readily conducted landward than toward the well screen.

b) Corners. Where a levee bends or turns a corner (frequently encountered where a riverfront levee meets a flank levee), the landside toe is subject to seepage from two directions and the measured residual heads may be significantly higher than those predicted from the 2D analysis.

c) Back levees and flank levees. Where levees are built to provide protection from small creeks and streams traversing the main river valley that are not efficiently connected to the pervious substratum, piezometric levels may reflect slowly rising regional groundwater levels rather than being a function of the variables involved in under seepage analysis.

d) Entrance and exit distances. Entrance and exit distances calculated at piezometer ranges were frequently found to be shorter than assumed for the original design. Where values of 180 to 300 m were assumed in design, measured values were often 120 m or less.

e) Permeability ratio. The ratios kr/kb were smaller than assumed for design (400 to 2,000) [4] but were reasonably consistent with later design guidance (100 to 800 in Rock Island) [5].

Occurrence of sand boils. Sand boils occur at less-than-predicted gradients. This was noted as early as 1952 and is well documented in Figure 20 taken from [21]. It was also noted by [5] in his analysis of Rock Island performance data. Nevertheless, boil occurrence is rare in terms of the many kilometres of levee subjected to similar gradients. It is apparent that local geologic conditions must have a more significant influence on where boils occur than does the gradient. There is considerable evidence that boil occurrence is often related to concentration of seepage at discontinuities and defects in the top blanket. Such non-uniform blanket geometry is not accounted for in the uniform, 2D model used for design. Despite the discussion concerning geologic conditions in [20] and the 3D cross sections illustrating floodplain deposits (Figure 9) and their relationship to under seepage, the same analysis and design criteria are applied in the same manner for all types of deposits.

Relationship of boils to blanket thickness. The correlation presented by [5] between boil occurrence and top blanket thickness implies that boils are the only concern and overlooks the possibility of rather sudden rupture of thick clay blankets retaining high piezometric pressures (heaving). This was apparently the case of the 1943 floodwall failure at Claryville, MO, described by [13].

Critical Gradient Criteria. [5] notes that the calculation of the critical gradient was based on a homogenous top blanket with no cohesion and flexural strength and noted that these assumptions would often be invalid. This was also challenged in a discussion of [19]. This discussion recommended the use of a factor of safety against uplift defined as the ratio of the saturated weight of the blanket to the piezometric pressure at the base of the blanket.

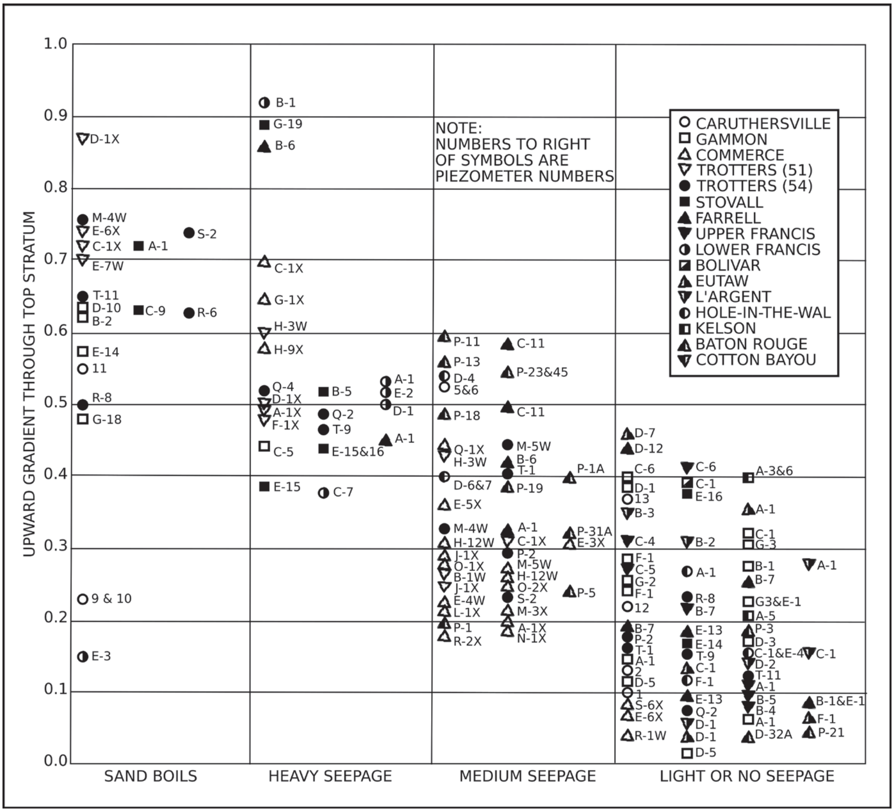

Figure 20. Degree of seepage vs. upward gradient for many levee locations [12]

Calculation of gradients. As pointed out by [5], the calculation of gradients is an uncertain process because of the difficulty in properly estimating the blanket thickness. It becomes very judgmental where a non-homogeneous blanket must be transformed to an equivalent homogeneous blanket, or where the blanket changes thickness along or beyond the levee toe. In ridge and swale topography, the top blanket may be highly stratified, and development of an idealised design profile by the engineer may seem to be a meaningless process.

Calculation of entrance and exit distances and residual head. The review of [5] suggested that accurate values of the entrance distance, X1 and the exit distance, X3 are almost impossible to obtain. The problems are not as severe in practice as it would appear, even though they are functions of four uncertain parameters. This arises because the prediction of interest is the residual head, at the levee toe. Working backwards through the analysis equations, h0 is determined by simple proportion involving the entrance and exit distances:

It is apparent that h0 can be accurately calculated if the proportion between X1 and X3 is reasonably correct, even if their actual values are grossly in error. For a levee reasonably distant from the river, where riverside values of the parameters are used to calculate X1, and landside values are used to calculate X3. As the landside and riverside values are often significantly correlated, the equations yield values for the entrance and exit distances that are generally in correct proportion. Furthermore, the extraction of the square root tends to minimise the effects of error in the parameters, and errors in z and d are just as likely to be compensating as biased. [4] implies the same idea; that is, that one can reasonably predict the residual head even with the wrong permeability ratios.

Permeability values and ratios. Although hydraulic conductivity (or permeability) is difficult to quantify, the Corps' recommendations are not arbitrary as suggested by [5] but are based on considerable experience and piezometric measurements. Residual heads and gradients are dependent only on the ratios of the permeabilities, not their absolute values. As the values used are back calculated from observed piezometric grade lines and then reused in the same equations to estimate the piezometric grade line for other conditions, it is not surprising that they provide generally good results. The permeability ratios and the blanket formulas form a closed loop; thus, they tend to work whether they are correct or not.

Nevertheless, data obtained from the 1973 flood in St. Louis indicated lower ratios than those typically recommended for use in the Lower Mississippi Valley, and the Rock Island analysis indicated still lower values. While the reasons for this trend require more study, it is noted that these sites represent significant differences in the geologic environment. The Lower Mississippi is a classic meandering stream in a wide valley. Levees are at relatively great distances from the river, and discontinuities such as clay plugs, and oxbows are common. The river carries a high sediment load. At the other extreme, the characteristics of the valley in the Rock Island District are primarily related to glacial melting. The valley is rather narrow and there are relatively few meander deposits. Levees are relatively close to the river. Much of the sediment load enters the river downstream of the Rock Island District. The St. Louis District and the Middle Mississippi Valley represent transitional conditions. Concentrations of seepage adjacent to clay plugs or other blanket discontinuities increase residual heads and may result in apparently higher permeability ratios than would be measured under relatively uniform blanket conditions.

Determination of parameters from piezometer data. Estimates of entrance distances, exist distances and permeability ratios have generally been made only at piezometer ranges because a linear hydraulic grade line can be fitted through a number of points. Too many assumptions appear necessary to estimate these factors from a single piezometer at the levee toe. However, all reports of such analyses have mentioned the difficulty in obtaining reasonable values because of the sensitivity of the calculations to minor errors in the differences between piezometer readings.

Using simplified equations and the measured residual head from a single piezometer at the levee toe, and making a few reasonable assumptions, considerable insight can be gained regarding the probable values of X1, X3 and the permeability ratio.

Deficiencies in procedures, summary. Based on the various reviews of performance data, a summary of the assumptions made in under-seepage analysis and the special cases in which they may be deficient has been summarised. The performance data also indicate that there can be a wide variation in the observed values of parameters assumed or calculated in the design. Possible improvements to the analysis procedures lie in four areas:

a) Computerised analysis using existing procedures to allow more expedient solutions.

b) Probabilistic adaptation of existing procedures to allow for uncertainty in the parameters.

c) Extension of the existing procedures to more general cases to allow more realistic modelling of actual conditions.

d) Improvements in the exploration process to allow better identifications of the subsurface conditions to be modelled.

e) The equations for seepage analysis as well as for design of seepage berms and relief wells have been adapted to computer programs by several parties.

Slope stability

Dams and levees are particularly sensitive to slope stability problems. This is because of seepage as well as other site factors which tend to magnify small problems. Shown in Figure 21a are terms related to landslides in general and Figure 21b shows a typical slope failure on the downstream side of a dam. One must first realise that the slope is seeking a better equilibrium point by sliding, so if the material at the toe is removed, more sliding will occur. Another important point is that the slope forces are very large and structural elements such as stabilising piles or walls generally will not help. On a hillside or natural slope there is often firm ground or rock behind the surficial soils that will provide an anchoring point for tiebacks and supports. Of course, in an embankment, such support is not available. Additionally, seepage from the waterside, rainfall erosion, animal activity or differential settlement of the embankment may all encourage instability.

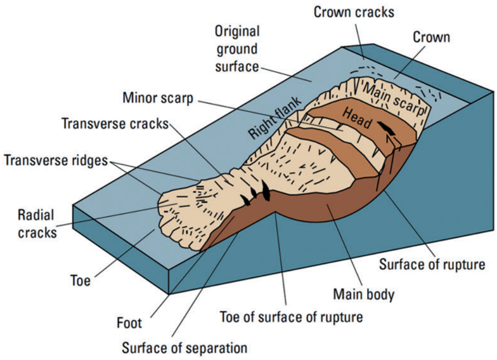

(a)

(b)

Figure 21. (a) Landslide terminology and (b) typical slope failure on the downstream side of the dam [9]

Evaluating slope stability

The numerical evaluation of slope stability requires calculating two competing elements: 1. The forces (or rotational moments) driving the slope downward; and 2. The forces (or rotational moments) resisting the downward movement. The driving forces originate from the weight of soil and water in the slope while the resisting forces come from the soil's strength, usually expressed as cohesion (c) and friction (ϕ).

Infinite and finite slope analysis

The simplest and most useful analysis assumes the slope to be infinite in length and the slide to be rather shallow in depth. The calculation of stability is straightforward and gives a first approximation of the stability of the embankment. Figure 22a, b shows two scenarios where the first is a dry slope (no water action) and the second accounts for seepage forces moving down the slope. This may occur if there is seepage near the surface of the downstream face, and also if the reservoir or upstream water drops suddenly, leaving pore water trapped in the soil because the soil itself cannot drain fast enough. "Suddenly" is a relative term, depending on the hydraulic conductivity of the soil in the slope. Gravels and sands might drain in minutes or a day. Silts would take several days to several weeks, and clays may take six months. So sudden drawdown for a clay embankment would be anything faster than a few months.

The factor of safety for stability is the ratio of resisting forces (soil strength expressed as (c, ϕ)) to the action forces (downward weight of the soil (γ), and seepage or water forces if present). One could formulate equilibrium of the system as shown in the equations below each section. Both equations have the resisting forces on top and action forces on the bottom. If the safety factor is less than 1.0, the slope will fail by sliding downhill. For the dry conditions, the contributions of cohesion and friction angle are separated. For sandy slopes (c=0), the slope remains stable if it is flatter than ϕ' For the same sandy slope with seepage occurring, the effect of the water reduces resistance and increases actions.

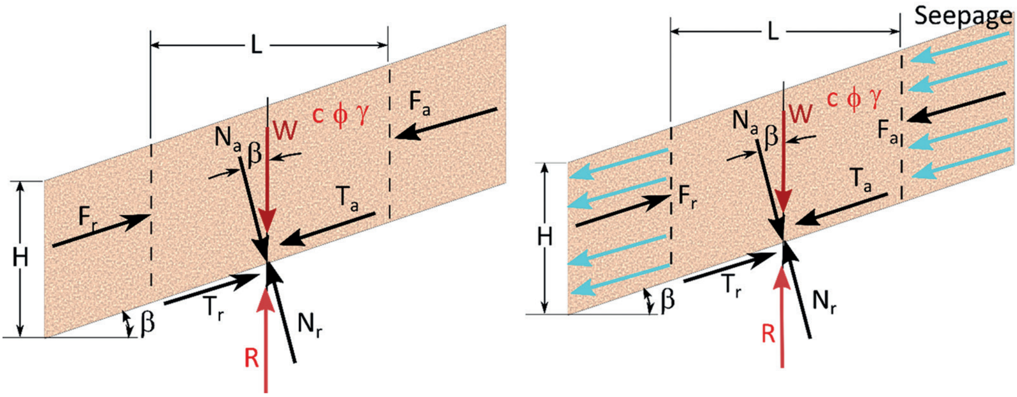

$$SF = \frac{c'}{\gamma H \cos^2 \beta \tan \beta} + \frac{\tan \phi'}{\tan \beta}$$

$$SF = \frac{c'}{\gamma_{sat} H \cos^2 \beta \tan \beta} + \frac{\gamma' \tan \phi'}{\gamma_{sat} \tan \beta}$$

(a) *(b)*

Figure 22. Infinite slope forces for (a) dry conditions and (b) seepage conditions (compiled by the author)

Typically, $\gamma_{sat} \approx 2 \times \gamma'$ and the tangent of the slope ($tan\beta$) must be less than 1/2 ($tan\phi'$). Infinite slopes fail along a shallow plane below the surface. Sandy materials will often fail this way. However, materials that are mixed sand and clay ($c,\phi \neq 0$) experience more deep-seated failure. The weakest surface where failure takes place may be irregular, but more circular than planar. In order to better model such failures, the method of slices is often used. The approach first assumes a failure plane through the embankment which may be circular but does not have to be. The mass of soil above the failure plane is then divided into slices (Figure 23) and forces acting between each slice are considered. Rotational equilibrium is considered here so resisting moments due to soil strength and acting moments due to soil weight are considered. Note that some of the soil weight will produce a negative rotation (slices 1–4). The soil at the base of each slice is resisting rotational movement (S_i in upper diagram) while the larger slices are acting to de-stabilise the slope (slices 5–10). The computation for this example is moderately complex; I used a spreadsheet to perform the calculation and I spent less than an hour setting it up, computing and displaying the results in Excel. The computational procedure is iterative: you must guess the eventual factor of safety before you compute it. The final solution converges after 2 or 3 intelligent guesses. This analysis produced a factor of safety = 1.5. As with most geotechnical analyses, two or three digits of precision is as accurate as one can compute since there are so many uncertainties about soil strength, layer geometry and pore pressure conditions. Since this is only one possible failure surface, a full analysis would try other circles with different centre points and different radii, compute factors of safety and select the candidate with the lowest value. Obviously, a software model is normally used to perform stability analyses. The same danger with sudden drawdown or seepage forces applies here as it did before with the infinite slope analysis. The soil is heavier and weaker during those conditions; therefore, it must be carefully modelled and checked as part of the embankment stability assessment.

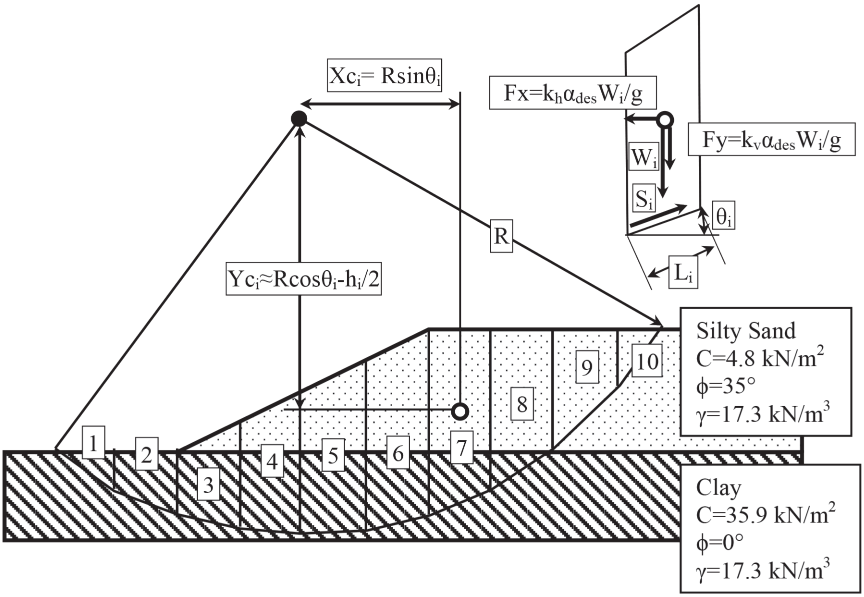

Figure 23. Slope stability by method of slices (compiled by the author)

Note that the upper diagram shows forces acting on one slice. Trial failure surface cuts through two different layers of soil

Software program for slope stability

Slope stability analysis by limit equilibrium methods, such as the one presented in Figure 23, are the standard approach to determine a factor of safety against sliding. Soil properties, layer geometry, boundary conditions and limits on the number of possible failure surfaces to attempt are input to the model analysis. The software will test perhaps 100 trial surfaces and return the worst (lowest FS) 20 or so. A typical output is shown in Figure 24. The yellow fence is the slices used by the software to compute the stability problem in a manner similar to Figure 23. The other red lines are other failure surfaces where FS = 1.9 to 2.0. There were over 100 trial surfaces in the analysis; however, these few give a good enough impression about how it searches for solutions.

The finite element method can be used to examine slope stability as well; however, a different approach is required. Since FEM is a continuum approach, there will not be a sharp failure surface where sliding takes place. Instead, a strength reduction method is used where the strength of materials are reduced until a prescribed level of strain occurs. The level of strain is enough to indicate impending failure, but not enough to cause the numerical computation to become unstable. Figure 25 shows a 3D problem with finite element mesh. There are 43,000 nodes with about 120,000 equations and unknowns and a total of about 13,000 elements. The execution time was 41 minutes on a high-performance workstation. The displacement surface is shown and has a shape similar to a circular failure arc. Based on the strength reduction method, the factor of safety is 0.97.

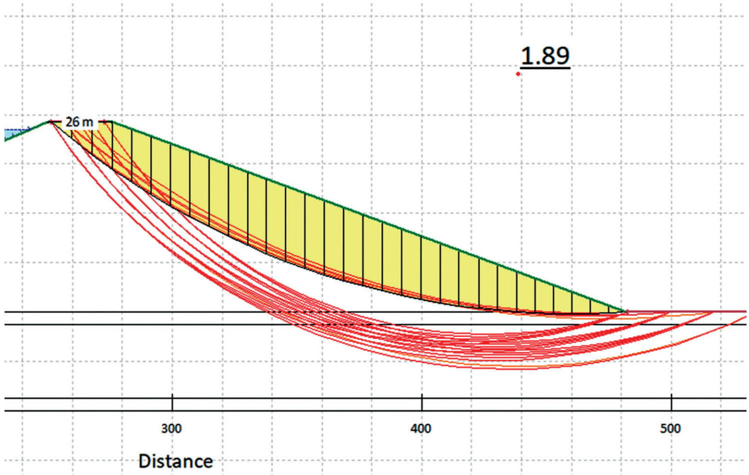

Figure 24. Slope stability analysis showing critical failure surface and slices used to compute FS = 1.89 (analysis by author using [8])

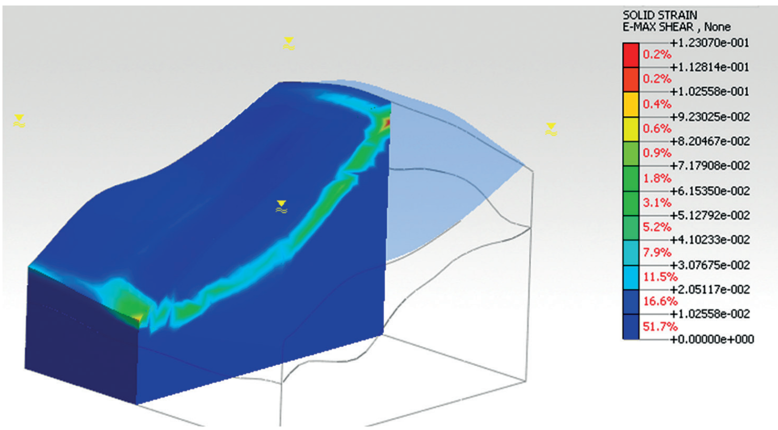

Figure 25. 3D view of maximum shear strains during strength reduction FS = 0.97 (analysis by author using [12])

Conclusions

Soil mechanics is indeed a complex system of natural materials and forces. Predicting behaviour due to flooding or other extreme events is even more difficult. At the present time, the level of sophistication in analysis outstrips the level of accuracy of data and known boundary conditions. Engineers and water resource managers are cautioned that wonderful 3D renderings do not make an analysis any more accurate. Careful observation and measurement in the field during flood events are still the best resource for better management and engineering.

References

[1] Bennett PT (1946). The Effect of Blankets on Seepage through Pervious Foundations. Trans. Am. Soc. Civ. Eng. Jan;111(1):215–252. DOI: https://doi.org/10.1061/TACEAT.0005902

[2] Boulanger RM, Duncan JM (s. a.). Geotechnical Engineering Photo Album. Available from: https://research.engineering.ucdavis.edu/gpa/.

[3] Chadwick WL, Casagrande A, Coombs HA, Dowd MW, Fucik EM, Higginson RE, Leps TM, Peck RB, Seed HB, Jansen RB (1976). Report to U.S. Department of the Interior and State of Idaho on Failure of Teton Dam. Washington D.C.: U.S. Government Printing Office.

[4] Cunny RW (1980). Documentation and Analysis of Rock Island Underseepage Data. Technical Report GL-80-3. U.S. Army Engineer Waterways Experiment Station. Vicksburg, MS.

[5] Daniel DE (1985). Review of Piezometric Data for Various Ranges in the Rock Island District. Report to U.S. Army Corps of Engineers Waterways Experiment Station. Vicksburg, MS.

[6] Das BM (2021). *Principles of geotechnical engineering*. Cengage learning.

[7] Estrela T. Hydraulic Modelling of the Tous Dam Break. In: Alcrudo F, Morris M, Fabbri K editors. Fourth CADAM (Concerted Action in Dam Break Modelling). Workshop, Zaragoza, Spain; 1999. Published by the European Commission.

[8] Geostudio Software (2021). Available from: www.geoslope.com/

[9] Highland L (2004). Landslide types and processes. USGS FS-2004-3072. Available from: https://pubs.usgs.gov/fs/2004/3072/fs-2004-3072.html

[10] Kieffer SW (2011). Missouri levee boil forces evacuations. Available from: www.geology-inmotion.com/2011/06/missouri-levee-boil-forces-evacuations.html

[11] Meehan CL, Benjasupattananan S (2012). An Analytical Approach for Levee Underseepage Analysis. J Hyd. Nov;470–471:201–211. Available from: www.sciencedirect.com/science/article/pii/S0022169412007299 DOI: http://dx.doi.org/10.1016/j.jhydrol.2012.08.050

[12] Midas IT (2018). Midas GTS NX Geotechnical Engineering Finite Element Analysis Software. Available from: www.midasgeotech.com/solution/gtsnx

[13] Middlebrooks TA, Jervis WH (1947). Relief Wells for Dams and Levees. Trans Am Soc Civ Eng. 112(1):1321. DOI: https://doi.org/10.1061/TACEAT.0006047

[14] Office of the State Engineer (1983). An investigation of the failure of the Lawn Lake Dam. Larimer County, Colorado. p. 31.

[15] Park J, Santamarina JC (2017). Revised Soil Classification System for Coarse–Fine Mixtures. J Geo Geoenv Eng. 143(8). DOI: https://doi.org/10.1061/(ASCE)GT.1943-5606.0001705

[16] Peter P (1982). Canal and River Levées. New York: Elsevier.

[17] Seed HB (1971). Personal photos. Available from: http://damfailures.org
[18] Sharma RP, Kumar A (2013). Case Histories of Earthen Dam Failures. Seventh International Conference on Case Histories in Geotechnical Engineering. Paper No. 3.03a. p. 6.
[19] Turnbull WJ, Mansur CI (1959). Investigation of Underseepage – Mississippi River Levees. J Soil Mech Found Div Apr;85(4). DOI: https://doi.org/10.1061/JSFEAQ.0000215
[20] USACE (1956). Investigation of Underseepage and Its Control. Lower Mississippi River Levees. Technical Memorandum 3-424. U.S. Army Corps of Engineers Waterways Experiment Station. Vicksburg, MS.
[21] USACE St. Louis (1976). Reevaluation of Underseepage Controls, Mississippi River Levees, Alton to Gale, Illinois, Phase I: Performance of Underseepage Controls during the 1973 Flood.
[22] USACE (1993). Seepage Analysis and Control for Dams. Engineering Manual 1110-2-1901. U.S. Army Corps of Engineers. p. 392.
[23] USACE (2000). Design and Construction of Levees. Engineering Manual 1110-2-1913. U.S. Army Corps of Engineers. p. 164.
[24] US Bureau of Land Reclamation (1976). Teton Dam. Available from: www.usbr.gov/pn/snakeriver/dams/uppersnake/teton/5.html
[25] Wolff TF (1989). Levee Underseepage Analysis for Special Foundation Conditions. Research Report REME-GT-11. U.S. Army Corps of Engineers Waterways Experiment Station. Vicksburg, MS.
[26] Zhang LM, Xu Y, Jia JS (2007). Analysis of Earth Dam Failures – A Database Approach. ISGSR2007, First International Symposium on Geotechnical Safety and Risk. Shanghai, China. p. 11.